Turkish Journal of Electrical Engineering & Computer Sciences

http://journals.tubitak.gov.tr/elektrik/

Research Article

Turk J Elec Eng & Comp Sci
(2019) 27: 1667 – 1679

doi:10.3906/elk-1807-93

A hybrid of tropical-singular value decomposition method for salt and pepper noise removal

Achmad ABDURRAZZAQ[1,*], **Ismail MOHD**[2], **Ahmad Kadri JUNOH**[1], **Zainab YAHYA**[1]
[1]Institute of Engineering Mathematics, Universiti Malaysia Perlis, Kampus Pauh Putra, Arau, Perlis, Malaysia
[2]Laboratory of Computational Statistics and Operations Research, Institute for Mathematical Research, Universiti Putra Malaysia, Serdang Selangor, Malaysia

Received: 10.07.2018 • **Accepted/Published Online:** 10.03.2019 • **Final Version:** 15.05.2019

Abstract: The unknown information contained in an image that causes the change of information in the image is called noise. In this paper, we propose a new method for removing salt and pepper noise by using singular value decomposition and the concept of tropical algebra operations. To determine the performance of the proposed method, 20 test images are used as samples. Then three different image quality assessments are used: peak signal-to-noise ratio (PSNR), structural similarity (SSIM), and image enhancement factor (IEF). In addition, six different filtering methods, i.e. MF, DWMF, PSMF, MDBUTM, NAFSM, and BPDF, are used to compare the performance of the proposed method. The experimental results show that the proposed method yields better results than the existing methods, in particular the BPDF filtering method.

Key words: Noise removal, salt and pepper noise, impulse noise, singular value decomposition, tropical algebra

1. Introduction

In this era of technology, almost all aspects of life are related to digital items and tools such as smartphones, which are the primary needs nowadays. This condition triggers the emergence of various technological phobias (tech phobias) that we may never realize that we also have, such as nomophobia ("no mobile phone phobia"), loremophobia, or selfiephobia [1, 2]. An image is a form of communication that we always used to interact with others, whether directly or indirectly. Using images to communicate with others is common today, supported with the convenience of having a camera in smartphones. Images are widely used as a medium of communication because much important information can be obtained from an image. Images have digital values called picture elements, abbreviated to pixels, and these represent the content of the information in the image. By performing image processing, the information in images can be extracted. There are various types of image processing that have different functions and purposes, such as image filtering, image clustering, image segmentation, image watermarking, edge detection, and image recognition.

As mentioned earlier, the picture element (pixel) represents the information contained in images. Such information may be subject to interference due to unknown information contained in the image. This causes information alteration in the image and the condition of this information alteration is called noise. Noise is the random variation of the intensity of the image and appears as dirt spots in images. Noise can also be said to be the corrupted pixels of the image. Noise is usually generated during image capture. There are various factors that cause noise in an image. The cause of the emergence of noise in general is i) the imaging sensor

*Correspondence: razzaq.ganesha@gmail.com

being interrupted while taking the image, ii) excessive or less light intensity during image capture, and iii) the presence of dirt or dust on the camera lens [3–5].

Image denoising is a preprocessing stage aimed at removing noise from the corrupted image. Image denoising plays an important role in image processing, because image processing requires good-quality images with the same information as the original condition. In addition to eliminating noise we also need to maintain the undamaged image during the process of filtering. Over the years, research works have been done for image filtering in order to obtain the best image filters. The median filter is the filtering technique that continues to be developed so far. Some modifications of the median filter are widely known, including adaptive median filters, switching median filters, weighted median filters, and directional weighted median filters [6, 7]. By hybridizing the concepts of fuzzy and switching median filters we can improve the advantages of the switching median concept and this method is known as the noise adaptive fuzzy switching median filter (NAFSM) [8]. In 2011, a new filtering method by combining the concept of median and mean filter by considering the number of noisy pixels in the tested neighborhood, known as the modified decision-based unsymmetrical trimmed median filter (MDBUTMF), was introduced [9, 10]. NAFSM and MDBUTMF provide visual results with clear edges, but recovery image textures become blurred. To overcome these drawbacks, a new filtering method for low noise density, known as based on pixel density filtering (BPDF), was introduced in 2018, but BPDF only works well at 10% and 20% noise densities, and its effectiveness statistically decreases at 30% to 50% [11]. In this study, a new method in image denoising aimed at eliminating noise from images is proposed. The proposed method utilizes the concept of tropical algebra and matrix decomposition. Matrix decomposition will be used for noise detection and noise removal, and then the concept of tropical algebra will be used to optimize the pixel restoration process. The rest of the paper is organized as follows. In Section 2, some preliminaries will be discussed. In Section 3, the methodology used in this study will be explained. The results of the study are given in Section 4. Finally, in Section 5, the conclusion of this study will be explained.

2. Preliminaries

The basic ideas of the minimax theory, which is the basis of research in tropical algebra today, were introduced in [12]. Tropical algebra is an algebraic structure formed from real numbers equipped with two binary operations, namely maximum (respectively minimum) and addition, algebraically denoted as $(\mathbb{R} \cup -\infty, \oplus, \otimes)$ $(respectively \quad (\mathbb{R} \cup \infty, \bar{\oplus}, \otimes))$. Tropical algebra itself has an algebraic structure of semiring. In some research papers, sometimes the set of real numbers is augmented with $-\infty$ and in some cases also added with ∞. Some researchers called tropical algebra max-plus algebra specifically for the case of algebraic structures of real numbers added with $-\infty$ equipped with addition and maximum as the binary operations [13].

Tropical algebra is not a new topic, but it is still being developed. The works that have been done are mostly on the development of the existing concepts and used it to investigate the algebraic structure of tropical algebra [14–16]. The interesting thing is that recently there are many studies on tropical algebra, mainly about the applications of the tropical concept. Tropical algebraic geometry has been used to establish an algorithm in determining the common factor of multivariate polynomials. Solving the common factors problem is done by using an algebra-based computer program, i.e. Maple. By taking the tropical concept of building a solution algorithm, a more effective preprocessing method is obtained [17]. Tropical algebra can also be applied to cryptographic fields as platforms for cryptography. The use of the tropical algebra concept, rather than linear algebra, to build cryptographic algorithms is expected to strengthen security systems and close the gaps found in linear algebra [18].

The method of factoring one matrix into three matrices consisting of a diagonal matrix and orthonormal matrix is called singular value decomposition (SVD). Mathematically, SVD is denoted as follows:

$$A = UDV^T.$$

The matrix decomposition can facilitate data processing, because the result matrices from matrix decomposition contain important information from the original matrix. In computer science or computer engineering the matrix decomposition method is widely used in order to obtain some important information such as image processing or signal processing [19, 20].

In this paper, the template used as shown in Figure 1 means that singular value decomposition will be performed for the 3 × 3 matrix. Let matrix D be the diagonal matrix, the result of singular value decomposition, and *d(2,2)* are the second row and the second column entries of matrix D. The diagonal matrix holds control over the entries of matrix A. The variety of distribution values in matrix A is known through the entries of diagonal matrix D. In particular, the entry value of *d(2,2)* is highly sensitive to the value change in matrix A compared to other entries. *d(2,2)* will experience a significant exchange of value changer in matrix A; this property is then used to determine the lower limit (α_1) and upper limit (α_2) in the template with the same variation of values (noise-free template).

3. Procedure of the proposed method

The filtering process will run on the 3 × 3 template with point *p(i,j)* as the center. In general, the filtering process in this research consists of two stages. The first stage is the process of noise detection in noisy images. This is to make sure that the replacement process is only done on corrupted pixels, so that uncorrupted pixels can be maintained. In the second stage, if corrupted pixels are detected, the pixels will be changed to new pixels that have similar pixel values as the pixel values in the original images.

Stage 1: In this stage, the process of detecting noise in each pixel filtering process will be performed. In this research, noise detection uses singular value decomposition in the square matrix of size 3 × 3. The diagonal matrix obtained from the singular value decomposition result will be used for noise detection. Let *d(2,2)* be the second row entry and the second column of the diagonal matrix D. *d(2,2)* will be the indicator to determine the presence of noise on any 3 × 3 template in the noisy images based on the following inequalities:

$$\alpha_1 < d(2,2) < \alpha_2, \tag{1}$$

where α_1 and α_2 are parameters determined based on the presence of significant color change in the 3 × 3 templates.

The values of α_1 and α_2 are determined after doing a experimental quantitative analysis where the value will be set after the resulting images give the best performance. In this study we choose α_1 as 3 and α_2 as 8. However, the values of α_1 and α_2 can be any number as long as it is within this interval where the detection rate gives the best performance.

Stage 2: If noise is detected in the template, then image filtering will be done on the template. The steps of implementing the proposed filtering are as follows.

- Assume a 3 × 3 template with *p(i,j)* as the central pixel (Figure 1). Then the pixels surrounding *p(i,j)* are symmetric and defined as follows:

$$T=p(i+u,j+v),\ -1 \leqslant u,v \leqslant 1. \tag{2}$$

$(i\text{-}1, j\text{-}1)$	$(i, j\text{-}1)$	$(i\text{+}1, j\text{-}1)$
$(i\text{-}1, j)$	(i, j)	$(i\text{+}1, j)$
$(i\text{-}1, j\text{+}1)$	$(i, j\text{+}1)$	$(i\text{+}1, j\text{+}1)$

Figure 1. Pixel coordinates based on point *(i,j)*.

- First, 3 × 3 templates will be rearranged into a 4 × 2 array constructed by taking each two neighborhood pixels that are localized in the same line. Assume that *q(i,j)*, *i=1,2,3,4* and *j=1,2*, are the entries of the 4 × 2 array. In the first column the loads of value *q(i,j)* are smaller than or equal to the value in the second column added by β:

$$q(i,1) \leqslant q(i,2) + \beta, \tag{3}$$

where β is a constant indicating a change in color.

As long as the beta value is determined as a constant value, it will not change the resulting image. Here the beta value must be greater than 0. In this study we used 25 as a parameter that represents the value of beta. However, the value of beta can be any number as long as it has a value.

- Finally, the new pixel value is derived from the operation between the maximum of the first column and the minimum of the second column (Figure 2):

$$\widetilde{p}(i,j) = \left(\frac{\oplus_{i=1}^{4} q(i,1) \otimes \overline{\oplus}_{i=1}^{4} q(i,2)}{2} \right). \tag{4}$$

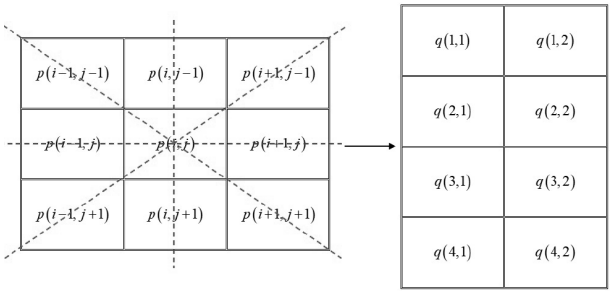

Figure 2. Illustration of determining the new pixel values.

If the maximum of the first column or the minimum of the second column is noise, then the procedure to determine the new pixel is as follows.

- The value *d(2,2)* is converted to 0 in order to obtain a new diagonal matrix. Then the matrices obtained from the singular value decomposition are multiplied again with the new diagonal D matrix, so that new 3 × 3 templates obtained with the distribution of values in the new template are more even and without any noise.

- Then the new 3 × 3 templates will be rearranged into a 4 × 2 array constructed by taking each two neighborhood pixels that are localized in the same line. Assume that *q(i,j)*, *i=1,2,3,4* and *j=1,2*, are the entries of the 4 × 2 array. In the first column the loads of value *q(i,j)* are smaller than or equal to the value in the second column added by β:

$$q(i,1) \leqslant q(i,2) + \beta, \tag{5}$$

where β is a parameter obtained based on the color changes.

- Next, determine the standard deviation of each row of the 4 × 2 array, namely sd_i, where *i=1,2,3,4*. In addition, from the standard deviation, the weight value w will be used to determine the new pixel value *p(i,j)*:

$$w = \overset{4}{\underset{i=1}{\oplus}} sd_i. \tag{6}$$

- Then choose the median value of each column of the 4 × 2 array, namely $\widetilde{q}_1$ and $\widetilde{q}_2$, so that the new pixel value *p(i,j)* is denoted as follows:

$$\widetilde{p}(i,j) = w \otimes \left(\frac{\widetilde{q}_1 \otimes \widetilde{q}_2}{2} \right). \tag{7}$$

4. Experimental results

In this section, the filtering results of the proposed method will be presented. The results will be compared with some other methods, i.e. standard median filter (SMF), directional weighted median filter (DWMF) [6], progressive switching median filter (PSMF) [7], noise adaptive fuzzy switching median filter (NAFSM) [8], modified decision-based unsymmetrical trimmed median filter (MDBUTM) [9, 10], and based on pixel density filter (BPDF) [11]. In order to measure the performance of the filtering algorithm, ten gray-scale images with 512 × 512 resolution (Figures 3a–3j) and ten gray-scale images with 256 × 256 resolution (Figures 3k–3t) will be used.

4.1. Image quality assessment

Three different evaluation criteria will be used to measure the performance of the filtering methods. First, the peak signal-to-noise ratio (PSNR) quantifies the image quality degradation, denoted as follows [11]:

$$PSNR(dB) = 10 \cdot \log_{10} \left(\frac{MAX}{MSE} \right), \tag{8}$$

where MAX is denoted as the largest value at gray-level of 255. MSE is mean-square-error, denoted as follows:

$$MSE = \frac{1}{MN} \sum_{i=0}^{M-1} \sum_{j=0}^{N-1} |q_{ij} - \widetilde{q}_{ij}|^2, \tag{9}$$

where $q_{i\,j}$ and $\widetilde{q}_{i\,j}$ are pixel values of the original image and recovery image. M and N are the size of the image.

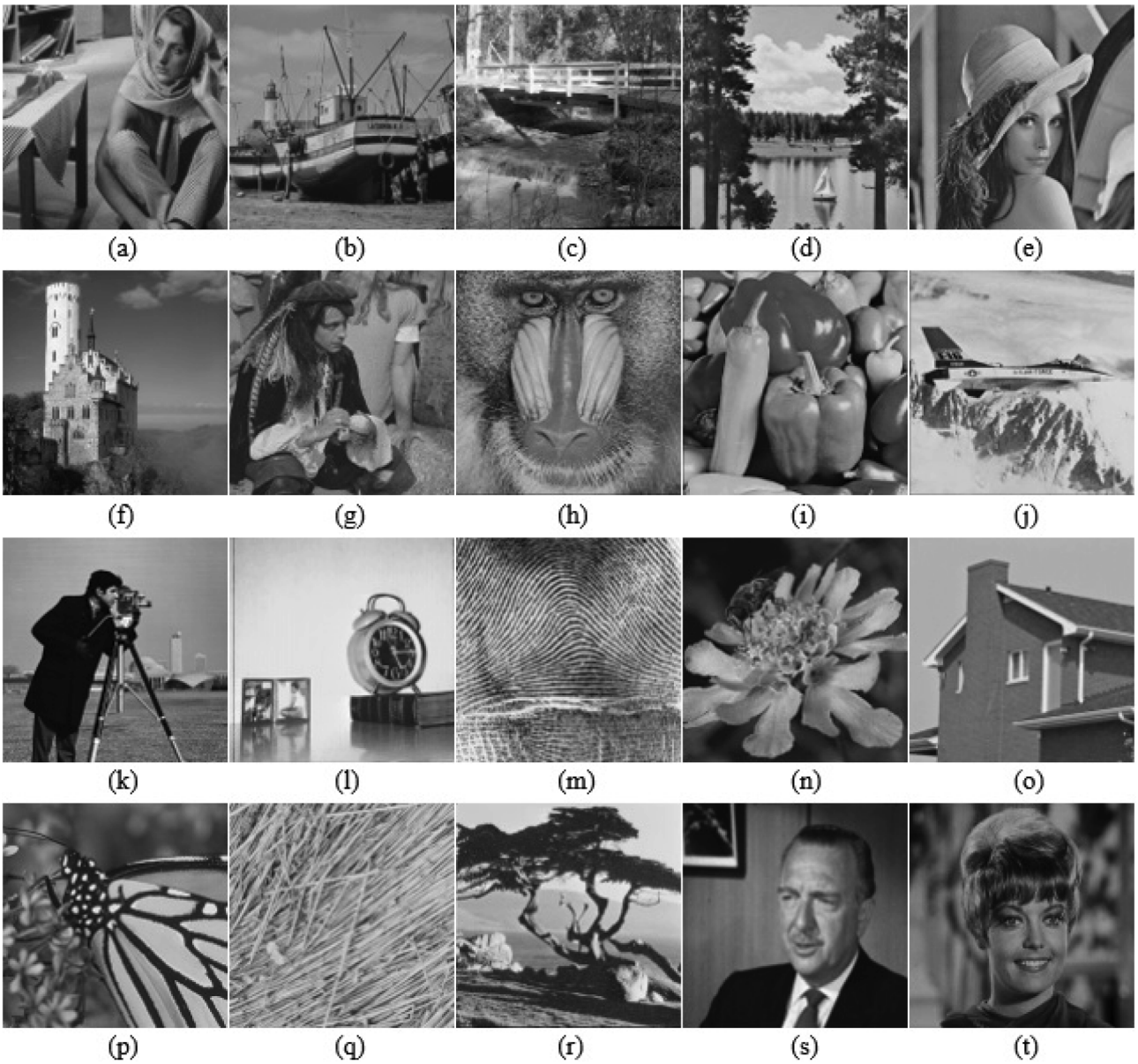

Figure 3. The original images. The first and second rows are 512 × 512 resolution: (a) Barbara, (b) boats, (c) bridge, (d) lake, (e) Lena, (f) castle, (g) man, (h) mandrill, (i) peppers, and (j) plane. The third and fourth rows are 256 × 256 resolution: (k) cameraman, (l) clock, (m) fingerprint, (n) flower, (o) house, (p) monarch, (q) straw, (r) tree, (s) Walter Cronkite, and (t) Zelda.

Secondly, the structural similarity index (SSIM) quantifies the similarity between two images, denoted as follows [21]:

$$SSIM = \frac{(2\mu_x\mu_y + C_1) + (2\sigma_{xy} + C_2)}{(\mu_x^2 + \mu_y^2 + C_1) + (\sigma_x^2 + \sigma_y^2 + C_2)}, \tag{10}$$

where μ_x, μ_y, σ_x, and σ_y are the average intensities, standard deviation, and covariance for the original image and recovery image.

Finally, the image enhancement factor (IEF) is denoted as follows [9]:

$$IEF = \frac{\sum_{i=0}^{M-1}\sum_{j=0}^{N-1}|q_{ij} - \widetilde{q}_{ij}|^2}{\sum_{i=0}^{M-1}\sum_{j=0}^{N-1}|p_{ij} - \widetilde{q}_{ij}|^2}, \tag{11}$$

where $q_{i\,j}$ is the original image, $\widetilde{q}_{i\,j}$ is the recovery image, and $p_{i\,j}$ is the noisy image. M and N are the size of the image.

4.2. Evaluation results

The filtering results of the proposed method quantitatively yield better results than the other methods, specifically better than the BPDF method. The results of the average calculation of PSNR, SSIM, and IEF for twenty test images are shown in Table 1. Based on Table 1, the proposed method works very well in every noise density compared to other methods.

Table 1. The mean results of the filtering of twenty images.

ND	Evaluation	MF	DWMF	PSMF	MDBUTMF	NAFSM	BPDF	Proposed
10%	PSNR	27.14	30.97	32.98	34.36	34.77	35.98	38.23
	SSIM	0.8031	0.9014	0.9387	0.9696	0.9747	0.9802	0.9859
	IEF	22.71	75.79	100.46	111.47	131.86	158.85	302.79
20%	PSNR	26.08	29.60	31.34	30.97	31.70	32.08	34.17
	SSIM	0.7783	0.8504	0.9263	0.9242	0.9486	0.9549	0.9670
	IEF	32.19	91.40	125.65	97.52	126.22	125.35	217.99
30%	PSNR	24.93	28.05	29.60	29.68	29.78	29.32	31.30
	SSIM	0.7423	0.7936	0.9078	0.9168	0.9205	0.9217	0.9408
	IEF	34.81	88.15	115.16	116.24	120.50	96.39	158.15
40%	PSNR	23.48	25.93	27.76	28.37	28.34	27.07	28.96
	SSIM	0.6839	0.7186	0.8760	0.8911	0.8898	0.8787	0.9039
	IEF	31.23	64.67	94.79	114.91	113.58	74.95	118.68
50%	PSNR	129.57	22.40	25.94	27.19	27.16	24.95	26.97
	SSIM	0.6003	0.6020	0.8335	0.8576	0.8560	0.8216	0.8543
	IEF	25.79	31.15	77.22	106.91	106.04	55.72	90.73

Table 1 shows that the average values of PSNR, SSIM, and IEF at 50% of the noise density of the proposed method are slightly lower than MDBUTMF and NASFM. This does not mean that the proposed method is unsuccessful at 50% of the noise density for each sample image. In Tables 2 and 3, the results of PSNR, SSIM, and IEF of the methods for 50% of the noise density are shown.

Next, some of filtering results will also be given visually. Figure 4 shows the recovery results of the mandrill image (Figure 4a), at 50% noise density (Figure 4b), and from MDBUTMF (Figure 4c), NAFSM (Figure 4d), BPDF (Figure 4e), and the proposed method (Figure 4f). In addition, Figure 5 shows the texture part of Figure 4, where the filtering result from the proposed method gives a better texture than the existing methods.

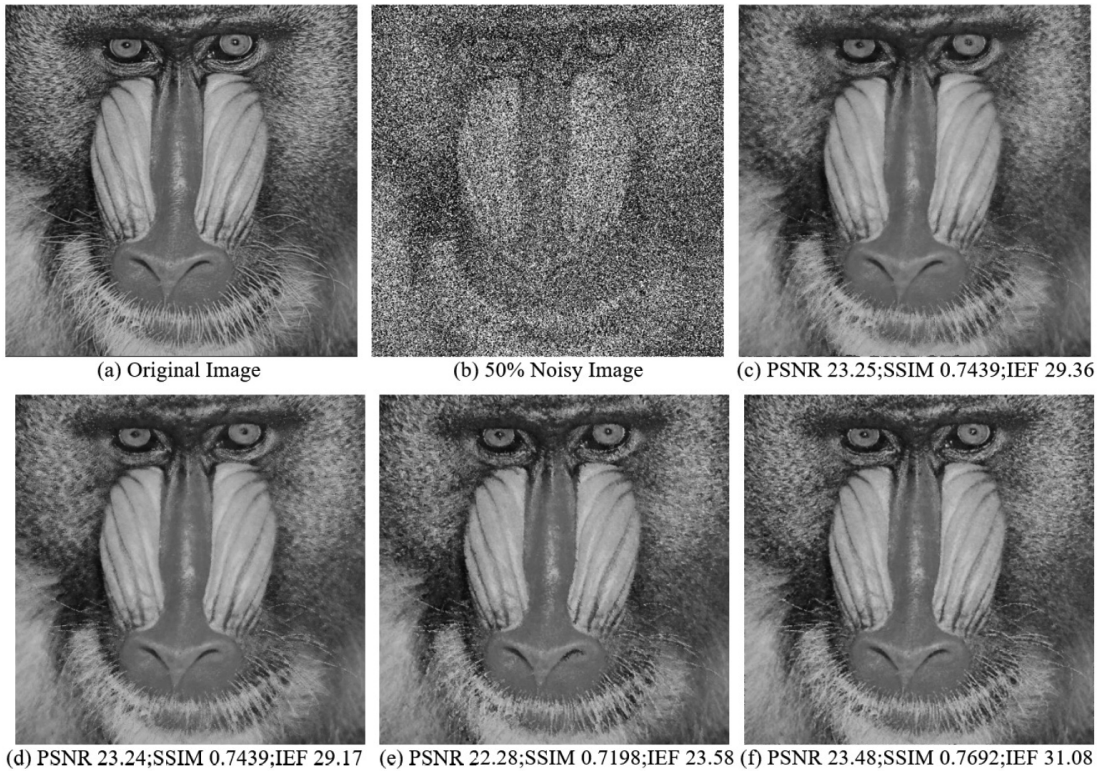

Figure 4. Filtering results of mandrill image: (a) original image, (b) noisy image, (c) MDBUTMF, (d) NAFSM, (e) BPDF, (f) proposed.

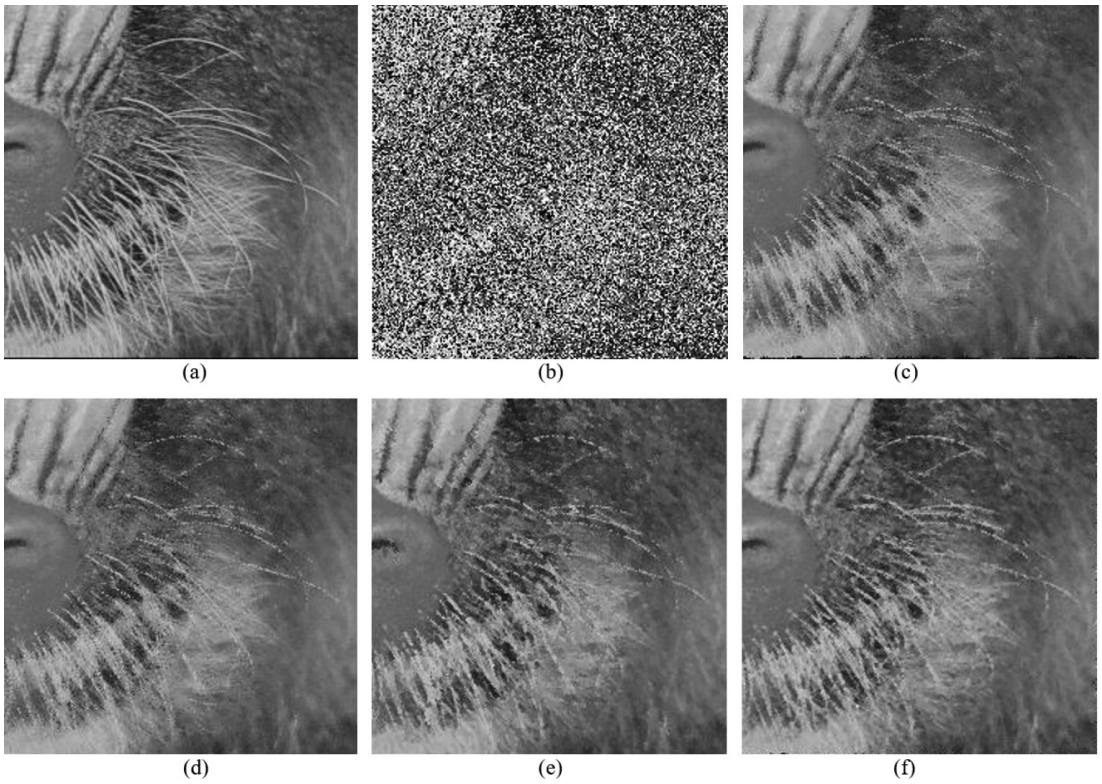

Figure 5. The textures of the filtering results from Figure 4: (a) original image, (b) noisy image, (c) MDBUTMF, (d) NAFSM, (e) BPDF, (f) proposed.

Figure 6 shows the filtering results of the proposed method used for some of the different noise densities. The Lena image is used for tests with three different noise densities; Figure 6a shows the filtering result of the noisy image with 10% noise density, Figure 6b the filtering result of the noisy image with 30% noise density, and Figure 6c the filtering result of the noisy image with 50% noise density. The proposed method successfully returns the noisy images, with different densities, to the original form without damaging the image.

Figure 6. Filtering results using the proposed image with three different noise densities.

As mentioned earlier, image denoising is a noise removal process in the corrupted image comprising noise detection and pixel recovery processes. The use of singular value decomposition as a noise detection method is aimed at tracking noise in all arrays in the 3×3 matrix, which is then performed by pixel recovery based on Eq. (4). The use of the concept of tropical algebra is aimed at obtaining pixel values that approach the original values, which are then used to convert the corrupted pixels in the image. In addition, besides being used for the singular value decomposition detection process, it is also used to generalize the distribution of the 3×3 matrix if the noise is detected in the 4×2 matrix. Furthermore, the integration of the two algebraic concepts works well for clearing noise in the corrupted image and producing good visual output (Figures 4f, Figure 5f, Figure 6a, Figure 6b, and Figure 6c) and quantitative output (Tables 1–3).

5. Conclusion

Noise removal or image denoising or image filtering is included in the image preprocessing process. Noise removal is aimed at fixing the corrupted image by filtering out every pixel of the image. In [11], the original images that were used were not provided. This makes it difficult for other researchers who want to compare their performance of the filtering methods using the same images.

Table 2. The experimental results of images with 512 × 512 resolution for 50% noise density.

ND	Evaluation	MF	DWMF	PSMF	MDBUTMF	NAFSM	BPDF	Proposed
Barbara	PSNR	21.22	21.14	23.91	25.76	25.77	24.14	25.18
	SSIM	0.5511	0.5812	0.7965	0.8476	0.8479	0.8043	0.8326
	IEF	19.64	19.37	36.59	56.07	55.97	38.51	48.97
Boats	PSNR	23.45	24.71	28.02	29.09	29.02	26.78	29.35
	SSIM	0.6483	0.6335	0.869	0.8879	0.8853	0.8531	0.8853
	IEF	31.75	42.55	92.24	116.78	114.58	68.49	123.49
Bridge	PSNR	20.73	21.2	23.87	24.89	24.67	23.45	25.26
	SSIM	0.4681	0.5838	0.7363	0.7716	0.7709	0.7418	0.7971
	IEF	17.81	19.7	36.43	46.29	43.69	32.93	47.5
Lake	PSNR	21.43	22.78	26.24	27.15	27.08	24.87	27.35
	SSIM	0.5971	0.594	0.8212	0.8545	0.854	0.8164	0.8475
	IEF	24.66	29.94	66.35	82.45	80.86	48.53	85.63
Lena	PSNR	24.53	25.82	29.65	31.01	31.02	28.37	30.76
	SSIM	0.675	0.6971	0.8814	0.9068	0.9074	0.8683	0.8907
	IEF	40.53	54.69	131.87	180.52	180.62	98.09	168.41
Castle	PSNR	23.25	23.27	26.98	27.56	27.59	26.64	28.03
	SSIM	0.6416	0.6544	0.8749	0.8898	0.8882	0.8754	0.8764
	IEF	30.51	30.66	72.11	82.42	82.98	66.57	91.83
Man	PSNR	23.59	24.91	27.84	29.07	29.06	26.86	29.03
	SSIM	0.6173	0.6841	0.8403	0.8652	0.8655	0.8308	0.8662
	IEF	32.78	44.89	88.61	116.87	115.55	69.71	114.71
Mandrill	PSNR	19.89	19.39	22.14	23.25	23.24	22.28	23.48
	SSIM	0.4056	0.5112	0.6972	0.7439	0.7439	0.7198	0.7692
	IEF	13.61	12.1	22.68	29.36	29.17	23.58	31.08
Peppers	PSNR	24.04	25.82	29.01	31.92	31.93	28.04	30.12
	SSIM	0.6571	0.6622	0.8568	0.9079	0.9067	0.8513	0.8744
	IEF	37.51	56.36	188.38	229.76	230.89	94.36	152.22
Plane	PSNR	22.91	24.01	28.1	29.02	28.96	26.73	29.11
	SSIM	0.6864	0.6178	0.8998	0.9139	0.9139	0.8824	0.8999
	IEF	31.66	40.87	105.11	130.16	127.62	76.35	131.9

Noise detection using singular value decomposition can detect the presence of noise thoroughly in 3 × 3 templates. Furthermore, if noise is detected, the filtering process is then carried out using the concept of operations in tropical algebra of maximum (respectively minimum) and addition. However, if noise is also detected in the neighborhood pixels, it will be filtered using singular value decomposition first before the pixel restoration process is performed. As described in Section 3, the filtering process of singular value decomposition uses entries from diagonal matrix *d(2,2)*. It aims to reduce the significant value of noise and make the distribution of values from the neighborhood pixels more even.

The proposed algorithm has been shown to improve the performance of the filter image both visually and quantitatively. Quantitatively, three image quality assessments are used to measure the performance of image

Table 3. The experimental results of images with 256 × 256 resolution for 50% noise density.

ND	Evaluation	MF	DWMF	PSMF	MDBUTMF	NAFSM	BPDF	Proposed
Cameraman	PSNR	20.51	20.16	23.89	24.5	24.63	23.47	24.89
	SSIM	0.6137	0.5062	0.8403	0.8713	0.8686	0.839	0.85
	IEF	17.61	16.17	38.03	44.21	45.52	34.86	48.26
Clock	PSNR	21.9	21.81	25.85	26.77	26.59	25.06	25.25
	SSIM	0.6958	0.3725	0.8929	0.9145	0.9116	0.8849	0.8583
	IEF	27.39	26.99	67.86	83.92	80.75	56.77	59.25
Fingerprint	PSNR	16.81	15.35	19.29	18.56	18.52	18.67	20.78
	SSIM	0.3762	0.477	0.7216	0.6388	0.6352	0.6961	0.7898
	IEF	6.99	4.95	12.42	10.41	10.38	10.74	17.49
Flower	PSNR	21.76	22.92	26.14	27.72	27.68	24.56	27.07
	SSIM	0.6425	0.6383	0.867	0.8961	0.8944	0.8365	0.8726
	IEF	23.13	30.21	63.13	92.12	90.57	44.13	78.66
House	PSNR	23.89	24.7	28.52	30.12	30.51	26.98	29.45
	SSIM	0.6624	0.6275	0.8647	0.9056	0.9096	0.8576	0.8695
	IEF	34.75	41.99	101.59	146.44	159.56	70.68	124.21
Monarch	PSNR	19.77	20.68	23.61	25.2	25.06	22.37	25.05
	SSIM	0.6472	0.723	0.8627	0.8965	0.8944	0.8345	0.8735
	IEF	14.12	17.32	34.24	49.03	47.71	25.7	47.56
Straw	PSNR	18.79	18.35	21.51	22.07	21.99	20.43	22.75
	SSIM	0.3988	0.5385	0.7097	0.7203	0.7142	0.6649	0.7737
	IEF	10.92	9.86	20.42	23.29	22.79	15.91	27.17
Tree	PSNR	19.85	20.02	23.52	24.97	24.87	22.67	25.08
	SSIM	0.5788	0.5539	0.8047	0.8461	0.8447	0.8011	0.8377
	IEF	15.36	16.11	35.87	50.29	48.85	29.43	51.25
Walter Cronkite	PSNR	23.98	25.91	30.42	33.29	33.25	27.76	30.87
	SSIM	0.7397	0.6457	0.9352	0.9523	0.9457	0.9099	0.9229
	IEF	40.02	61.81	176.01	339.86	334.37	94.47	193.31
Zelda	PSNR	24.82	24.95	30.22	31.92	31.67	28.87	30.63
	SSIM	0.7033	0.7383	0.8984	0.921	0.9171	0.8648	0.898
	IEF	45.08	46.45	154.42	227.88	218.39	114.55	171.74

filters, namely PSNR, SSIM, and IEF. Based on Tables 1–3, it can be seen that the proposed method has better performance compared to other filtering methods. In addition, Figure 5 shows that the proposed method of maintaining the texture of the image is much better than other methods even for 50% noise density.

Acknowledgment

The authors would like to thank Jurnal KALAM (Karya Lorekan Asli Ahli Matematik) Enterprise, Lot 3116, Jalan Pantai, Kampung Pengkalan Maras, Mengabang Telipot, 21030 Kuala Terengganu, Malaysia, for the motivation and financial support provided for this research.

References

[1] Carlisle PA. Nomophobia: A Rising Trend in Students (Addiction, Cell Phone Addiction). Scotts Valley, CA, USA: CreateSpace Independent Publishing Platform, 2017.

[2] Parasuraman S, Sam AT, Yee SWK, Chuon BLC, Ren LY. Smartphone usage and increased risk of mobile phone addiction: a concurrent study. International Journal of Pharmaceutical Investigation 2017; 7 (3): 125–131. doi: 10.4103/jphi.JPHI_56_17

[3] Boyat AK, Joshi BK. A review paper: noise models in digital image processing. Signal & Image Processing: An International Journal 2015; 6 (2): 63-75. doi: 10.5121/sipij.2015.6206

[4] Julliand T, Nozick V, Talbot H. Image noise and digital image forensics. In: Digital-Forensics and Watermarking: 14th International Workshop; 7–10 October 2015; Tokyo, Japan. Berlin, Germany: Springer Verlag. pp. 3-17. doi: 10.1007/978-3-319-31960-5_1

[5] Kaur G, Kumar R, Kainth K. A review paper on different noise types and digital image processing. International Journal of Advanced Research in Computer Science and Software Engineering 2016; 6 (6): 562-565.

[6] Dong Y, Xu S. A new directional weighted median filter for removal of random-valued impulse noise. IEEE Signal Processing Letters 2007; 14(3): 193-196. doi: 10.1109/LSP.2006.884014

[7] Wang Z, Zhang D. Progressive switching median filter for the removal of impulse noise from highly corrupted images. IEEE Transaction on Circuits and System II: Analog and Digital Signal Processing 1999; 46 (1): 78-80. doi: 10.1109/82.749102

[8] Toh KKV, Isa NAM. Noise adaptive fuzzy switching median filter for salt-and-pepper noise reduction. IEEE Signal Processing Letters 2010; 17 (3): 281-284. doi: 10.1109/LSP.2009.2038769

[9] Esakkirajan S, Veerakumar T, Subramanyam AN, Prem Chand CH. Removal of high density salt and pepper noise through modified decision based unsymmetric trimmed median filter. IEEE Signal Processing Letters 2011; 18 (5): 287-290. doi: 10.1109/LSP.2011.2122333

[10] Vasanth K, Kumar VJS. Decision-based neighborhood-referred unsymmetrical trimmed variants filter for the removal of high-density salt-and-pepper noise in images and videos. Signal, Image, and Video Processing 2015; 9 (8): 1833-1841. doi: 10.1007/s11760-014-0665-0

[11] Erkan U, Gökrem L. A new method based on pixel density in salt and pepper noise removal. Turkish Journal of Electrical Engineering and Computer Sciences 2018; 26 (1): 162-171. doi: 10.3906/elk-1705-256

[12] Cuninghame-Green R. Lecture Notes in Economics and Mathematical Systems (Vol. 1). Berlin, Germany: Springer-Verlag, 1979.

[13] De Schutter B, Heemels WPMH, Bemporad A. Max-plus-algebraic problems and the extended linear complementarity problem—algorithmic aspects. IFAC Proceedings Volume 2002; 35 (1): 151-156. doi: 10.3182/20020721-6-ES-1901.00513

[14] Bertram A, Easton R. The tropical nullstellensatz for congruences. Advances in Mathematics 2017; 308 (2017): 36–82. doi: 10.1016/j.aim.2016.12.004

[15] Izhakian Z, Rowen L. Congruences and coordinate semirings of tropical varieties. Bulletin des Sciences Mathematiques 2016; 140 (3): 231–259. doi: 10.1016/j.bulsci.2015.12.001

[16] Schmitz K. Generic tropical varieties on subvarieties and in the non-constant coefficient case. Journal of Algebra 2015; 439 (2015): 294–315. doi: 10.1016/j.jalgebra.2015.05.002

[17] Adrovic D, Verschelde J. Tropical algebraic geometry in Maple: a preprocessing algorithm for finding common factors for multivariate polynomials with approximate coefficients. Journal of Symbolic Computation 2011; 46 (7): 755–772. doi: 10.1016/j.jsc.2010.08.011

[18] Grigoriev D, Shpilrain V. Tropical cryptography. Communications in Algebra 2014; 42 (6): 2624–2632. doi: 10.1080/00927872.2013.766827

[19] Anton H, Rorres C. Elementary Linear Algebra with Applications. 9th ed. Hoboken, NJ, USA: John Wiley & Sons, 2005.

[20] Yanai H, Takeuchi K, Takane Y. Projection Matrices, Generalized Inverse Matrices, and Singular Value Decomposition. New York, NY, USA: Springer-Verlag, 2011.

[21] Zhou W, Bovik AC, Sheikh HR, Simoncelli EP. Image quality assessment: from error visibility to structural similarity. IEEE Transactions on Image Processing 2004; 13 (4): 600-612. doi: 10.1109/TIP.2003.819861